Ru-pphen units is occurring: these units are not in equilibrium even at high temperature.

A possible exception to the observation of no hopping at increased T may occur for $[Ru(pbpy)_3]^{2+}$. This complex demonstrates a significantly larger decrease in P with temperature than the previous two examples. Indeed, the full photoselection spectrum for this complex shown in Figure 5 is nearly invariant between 77 and 300 K with the exception that the region near P_{max} seems "clipped", as though some limiting P were being encountered at approximately $P = 0.16$. This reduced value of P is tantalizingly close to $P = 0.143$, which may be taken as evidence that hopping is beginning to compete efficiently with luminescence.

The smaller change in the energy of emission for this complex indicates that the effect of the solvent environment on this chromophore is smaller than some of the other complexes. Thus, the decrease in P_{max} by approximately 0.045 may in reality reflect the beginning of energy transfer in this molecule at 300 K.

To summarize, we must conclude that the multiple emitting chromophores of the tris complexes and the mixed-ligand species with near-degenerate ligand-localized states are not in a dynamic equilibrium at 77 K or even at significantly higher temperatures, though some evidence for the initiation of this process is found for $[Ru(pbpy)_3]^{2+}$ at room temperature.

Conclusion

The detailed photoselection study of molecules with near-orbital degeneracies has indicated that the oscillating pattern seen in the SSEmP spectroscopy of Ru-diimine tris complexes, which correlates with the emission spectrum, derives from the effects of a type of "heterogeneous" solvation of the chromophores. The ICC model indicates that this causes the localized emitting triplet state to couple in different degrees of localized and delocalized portions of the excited singlet manifold.

Related to this is the variation of the wavelength at which P_{max} occurs in the SSExP spectroscopy of the complexes as a function of detection wavelength. This indicates that luminescence in tris complexes does in fact derive from chromophores that are "heterogeneously" solvated. In mixed-ligand species, the observation of the same result but of larger magnitude due to the nonidentical nature of the chromophores supports the same conclusion. A rough estimate of the magnitude of heterogeneous solvation of 200-300 cm^{-1} was obtained by comparison of the mixed-ligand species with tris complexes. In no case is evidence available relating this solvation hetreogeneity to the mechanism of the localization. Both the solvent independence of P_{max}[1,2] and the time-dependent P_{max} data implicate an intrinsic mechanism as the source of the localization.

An increase in temperature has the effect of red-shifting the luminescence of most complexes dissolved in PMM plastic. However, this effect is apparently inconsistent with thermal equilibration between localized emitting states in complexes with multiple nondegenerate chromophores. Thus, the presence of a dynamic exciton hopping process in the excited state of these species appears unlikely, at least on the time scale of the luminescence (approximately 5 μs). This conclusion was supported by temperature-dependent photoselection data that indicated that P was relatively unaffected for the mixed-ligand complexes by an increase in temperature, other than the effects of a slight loosening of the solvent with increased T.

Finally, the study of mixed-ligand complexes has provided some insight into the nature of localization in Ru-diimine species, as well as the nature of the luminescence process in this series of materials.

Acknowledgment. Support of this research by the Army Research Office (RTP) is gratefully acknowledged.

Contribution from the Department of Chemistry, The University of North Carolina at Chapel Hill, Chapel Hill, North Carolina 27599-3290

MLCT Excited States. Role of the Hydrido Ligand in Hydrido Polypyridyl Complexes of Osmium(II) and Ruthenium(II)

Elise Graham Megehee and Thomas J. Meyer*

Received October 12, 1988

The photochemical and photophysical properties of the complexes $[M(bpy)_2(CO)X]PF_6$ (bpy = 2,2'-bipyridine; M = Os, X = H, D, Cl; M = Ru, X = H, D) are reported in 4:1 ethanol/methanol solution from 90 to 300 K. Metal to ligand charge-transfer (MLCT) excitation fails to induce metal hydride photochemistry, but oxidative or reductive quenching of $[Os(bpy)_2(CO)H]^{+*}$ does induce a net redox chemistry. There is no evidence for significant contributions to the emission spectrum nor to nonradiative decay by the ν(Os—H) mode. For the analogous complex of Ru, there is a significant ν(Ru—H) k_H/k_D kinetic isotope effect for nonradiative decay.

Introduction

There is an extensive chemistry of transition-metal hydrido complexes, and such complexes play an important role in many metal-catalyzed reactions.[1] An extensive photochemistry has also been reported, but it has generally been based only on product and quantum yield studies.[2] There is little insight in this area into excited-state dynamics, detailed photochemical mechanisms, or the nature of the excited state or states responsible for the photochemistry. In general, the complexes that have been studied do not absorb appreciably in the visible region, they require ultraviolet excitation, and they lack a clearly defined or well-established chromophoric base.

In contrast, the photochemical and photophysical properties of the metal to ligand charge-transfer (MLCT) excited states of

(1) For general reviews see: (a) Hlatky, G. G.; Crabtree, R. H. *Coord. Chem. Rev.* **1985**, *65*, 1. (b) Slocum, D. W.; Moser, W. R. Catalytic Transition Metal Hydrides. *Ann. N.Y. Acad. Sci.* **1983**, *415*. (c) Muetterties, E. L., Ed. *Transition Metal Hydrides*; Marcel Dekker: New York, 1971. (d) Bau, R., ed. *Transition Metal Hydrides*; Adv. Chem. Ser. 167; American Chemical Society: Washington, DC, 1978. (e) Collman, J. P.; Hegedus, L. S. In *Principles and Applications of Organotransition Metal Chemistry*; University Science Books: Mill Valley, CA, 1980; p 60.

(2) For general reviews see: (a) Ferraudi, G. J. *Elements of Organotransitionmetallic Photochemistry*; Wiley: New York, 1988. (b) Geoffroy, G. L. *Prog. Inorg. Chem.* **1980**, *27*, 123. (c) Geoffroy, G. L.; Wrighton, M. S. *Organometallic Photochemistry*; Academic Press: New York, 1979. (d) Geoffroy, G. L.; Bradley, M. G.; Pierantozzi, R. *Transition Metal Hydrides*; Adv. Chem. Ser. 167; American Chemical Society: Washington, DC, 1978; p 181.

0020-1669/89/1328-4084$01.50/0

polypyridyl complexes of Ru^{II} and Os^{II} are well established.[3] The results of temperature-dependent lifetime and spectroscopic studies have led to relatively clear insights into electronic structure, excited-state dynamics, and the roles of the energy gap and molecular vibrations in the deactivation of these states.[3-5] For example, it is known that the energy acceptor role in nonradiative decay is dominated by medium-frequency ν(bpy) ring-stretching modes.[6]

Complexes such as *cis*-$[(bpy)_2M(CO)H]^+$ ($M = Os^{II}$, Ru^{II}) have been reported.[7,12] They offer the possibility of combining the well-established MLCT excited-state properties of polypyridyl complexes of Os^{II} and Ru^{II} with the photochemical reactivity of the metal-hydride bond. We have undertaken a series of photochemical and photophysical studies on these complexes with three goals in mind: (1) to investigate the possible use of the MLCT chromophore as an intramolecular sensitizer of metal hydrido photochemistry in the visible region; (2) to utilize the well-established photophysical properties of the MLCT excited state to explore the photochemistry; (3) to search for a possible role for high-frequency ν(M—H) or ν(C≡O) modes in excited-state decay.

Experimental Section

Synthesis. The starting materials $(bpy)_2OsCl_2$,[8] $(bpy)_2RuCl_2\cdot H_2O$,[9] and $(bpy)_2RuCO_3\cdot H_2O$[10] were prepared by using literature methods. The salts $[(bpy)_2Os(CO)Cl](PF_6)$,[7a] $[(bpy)_2Os(CO)(OSO_2CF_3)](CF_3SO_3)$,[9] $[(bpy)_2Os(CO)H](PF_6)$,[9,11] $[(bpy)_2Os(CO)D](PF_6)$,[9] $[(bpy)_2Ru(CO)Cl](PF_6)$,[9] $[(bpy)_2Ru(CO)H](PF_6)$,[12] and $[(bpy)_2Ru(CO)D](PF_6)$[12] were prepared by using modifications of literature procedures.

Materials and Solutions. Solvents used in the photochemical studies were spectroscopic grade. They were obtained from Burdick and Jackson. Ethanol and methanol were each distilled over MgI_2 immediately prior to use. Samples were prepared in an inert-atmosphere drybox and then freeze–pump–thaw-degassed for at least four cycles (10^{-5} Torr) before sealing in 9-mm glass cells. Sample concentrations were used such that the absorbance at 436 nm was between 0.2 and 0.5.

Preparative Photolyses. Photolyses were performed under a positive nitrogen pressure in a water-jacketed photolysis cell by using a 250-W sunlamp and a 350-nm cutoff filter. Sample volumes were 200–300 mL. The amount of the starting salt was 25–50 mg.

Measurements. UV–visible spectra were obtained by using a Hewlett-Packard 8451A diode array spectrometer and 1-cm quartz cells at room temperature. Infrared spectra were acquired on a Nicolet 20DX Fourier transform infrared spectrometer at room temperature. Solution spectra were obtained in CH_2Cl_2 in 1-mm NaCl cells.

Emission Lifetimes. Emission lifetimes for $[(bpy)_2Ru(CO)H]^+$ and $[(bpy)_2Os(CO)Cl]^+$ were determined by 450-nm laser flash excitation by using a Molectron DL-200 tunable dye laser with a coumarin 452-nm dye pumped by a Molectron UV-400 pulsed nitrogen laser. The emission was monitored at right angles, dispersed by a 0.25-m Bausch and Lomb 33-66-79 monochromator, detected by a Hamamatsu R446 PMT, recorded by a Tektronix R7912 transient digitizer, and subsequently averaged and stored by using a PDP 11/34 minicomputer. For $[(bpy)_2Os(CO)H]^+$ and $[(bpy)_2Os(CO)D]^+$, emission lifetimes were obtained by using the second harmonic (532 nm) of a Quanta-Ray DCR Nd:Yag laser as an excitation source in order to obtain an adequate signal near room temperature. Reported lifetimes are the averaged result of 130–250 decay traces. They were obtained by a least-squares fit of the data to first-order decay plots of ln I vs time (I = emission intensity), which were linear for at least 3 lifetimes.

Variable temperature control for the emission and lifetime measurements was achieved by using a modified Janis Instruments Model NDT cryostat or a Lakeshore Cryotronics Model DRC 84C temperature controller.

Emission Spectra and Quantum Yields. Corrected emission spectra and quantum yields were obtained by using an SLM 8000 Series photon-counting spectrofluorimeter. Excitation wavelengths were 450 nm for $[(bpy)_2Ru(CO)H]^+$ and $[(bpy)_2Os(CO)Cl]^+$ and 530 nm for $[(bpy)_2Os(CO)D]^+$ and $[(bpy)_2Os(CO)H]^+$. For spectral fitting and quantum yield measurements, the emission spectra were digitized and converted to an abscissa linear in energy by using the method of Parker and Rees.[13] Quantum yields were measured at room temperature (25 ± 2 °C) in 1-cm^2 glass cells in 4:1 (v:v) ethanol/methanol on freeze–pump–thaw-degassed samples by using $[Ru(bpy)_3](PF_6)_2$ in 4:1 (v:v) ethanol/methanol as a standard ($\phi_{em} = 0.068$).[14]

Emission Spectral Fitting. Emission spectral profiles were fit to a modified version of the two-mode Franck–Condon analysis (eq 1), which has been described in detail elsewhere.[6a,b,8a,15] The fits were carried out

$$I(\bar{\nu}) = \sum_{\upsilon_M}\sum_{\upsilon_L}(E_{00} - \upsilon_M\hbar\omega_M - \upsilon_L\hbar\omega_L/E_{00})^3(S_M^{\upsilon_M}/\upsilon_M!)(S_L^{\upsilon_L}/\upsilon_L!) \times \{\exp[-4(\ln 2)(\bar{\nu} - E_{00} + \upsilon_M\hbar\omega_M + \upsilon_L\hbar\omega_L/\Delta\bar{\nu}_{1/2})]\} \quad (1)$$

on a VAX 11/780 computer. In eq 1, $I(\nu)$ is the emission intensity at energy $\bar{\nu}$ in cm^{-1}. The quantities υ_M and υ_L are the vibrational quantum numbers for the medium- ($\hbar\omega_M \approx 1250$–$1450$ cm^{-1}) and low-frequency ($\hbar\omega_L \approx 300$–$600$ cm^{-1}) acceptor modes, respectively. The medium-frequency mode is an average of contributions from seven bipyridine framework stretching modes.[6b] The low-frequency mode is an average of low-frequency metal–ligand stretches and ligand torsional modes.[6b] The quantities S_L and S_M are the electron-vibrational coupling constants, which are related to the difference in equilibrium displacement between the ground and excited states, ΔQ_e, as shown in eq 2. In eq 2 M is the

$$S = \tfrac{1}{2}(M\omega/\hbar)(\Delta Q_e)^2 \quad (2)$$

reduced mass and ω ($=2\pi\nu$) is the angular frequency. The quantity E_{00} is the energy of the $\upsilon_M^* = 0$, $\upsilon_L^* = 0 \rightarrow \upsilon_M = 0$, $\upsilon_L = 0$ transition between the ground and excited states in cm^{-1}. The quantity $\Delta\bar{\nu}_{1/2}$ is the full width at half-maximum (fwhm) for the individual vibronic contributors to the emission spectra profile.

An additional quantity that was calculated from the spectral fitting parameters was E_0. It is the band maximum for the first medium-frequency vibronic component ($\upsilon_M^* = 0 \rightarrow \upsilon_M = 0$) and is the energy quantity that is utilized later in energy gap law calculations of nonradiative decay rate constants. It was calculated from the spectral fitting parameters by using eq 1 and setting $S_M = 0$. The procedure generates a single Gaussian band, for which the full width at half-maximum is $\Delta\bar{\nu}_{0,1/2}$.[6c] When calculated in this way, $\Delta\bar{\nu}_{0,1/2}$ includes contributions to the bandwidth both from the solvent and from the low-frequency modes treated semiclassically.

The summations in eq 1 were carried out over five vibrational levels for the averaged medium-frequency mode and over 15 vibrational levels for the averaged low-frequency mode. In the fitting procedure, initial estimates for the vibrational spacings $\hbar\omega_M$ ($=h\nu_M$) were made from the resolved vibronic structure that appears in the emission spectra in low-temperature glasses. Initial estimates for E_{00}, $\hbar\omega_M$, and S_M were made directly from the low-temperature spectra. The quantity E_{00} was taken as the energy at one-fourth of the maximum intensity on the high-energy

(3) (a) Juris, A.; Balzani, V.; Barigelletti, F.; Champagna, S.; Belser, P.; von Zelewsky, A. *Coord. Chem. Rev.* **1988**, *84*, 85. (b) Meyer, T. J. *Pure Appl. Chem.* **1986**, *58*, 1193. (c) Ferguson, J.; Herren, F.; Krausz, E. R.; Maeder, M.; Vrbancich, J. *Coord. Chem. Rev.* **1985**, *64*, 21. (d) Meyer, T. J. *Prog. Inorg. Chem.* **1983**, 389. (e) Kalyanasundaram, K. *Coord. Chem. Rev.* **1982**, *46*, 159. (f) DeArmond, M. K.; Carlin, C. M. *Coord. Chem. Rev.* **1981**, *36*, 325. (g) Kemp, T. J. *Prog. React. Kinet.* **1980**, *10*, 301. (h) Whitten, D. G. *Acc. Chem. Res.* **1980**, *13*, 83. (i) Balzani, V.; Bolletta, F.; Gandolfi, M. T.; Maestri, M. *Top. Curr. Chem.* **1978**, *15*, 1. (j) Sutin, N.; Creutz, C. *Inorganic and Organometallic Photochemistry*; Adv. Chem. Ser 168; American Chemical Society: Washington, DC, 1978; p 1. (k) Crosby, G. A. *Acc. Chem. Res.* **1975**, *8*, 231.

(4) (a) Yersin, H.; Gallhuber, E. *Chem. Phys. Lett.* **1987**, *134*, 497. (b) Hensler, G.; Gallhuber, E.; Yersin, H. *Inorg. Chem.* **1987**, *26*, 1641. (c) Yersin, H.; Hensler, G.; Gallhuber, E. *Inorg. Chim. Acta* **1987**, *140*, 157.

(5) (a) Blakely, R. L.; Myrick, M. L.; DeArmond, M. K. *Inorg. Chem.* **1988**, *27*, 589. (b) Ferguson, J.; Krausz, E. *Chem. Phys. Lett.* **1986**, *127*, 551. (c) Ferguson, J.; Krausz, E.; Vrbancich, J. *Chem. Phys. Lett.* **1986**, *131*, 463. (d) Ferguson, J.; Krausz, E. *Chem. Phys.* **1987**, *112*, 271.

(6) (a) Poizat, O.; Sourisseau, C. *J. Phys. Chem.* **1984**, *88*, 3007. (b) Caspar, J. V.; Westmoreland, T. D.; Allen, G. H.; Bradley, P. G.; Meyer, T. J.; Woodruff, W. H. *J. Am. Chem. Soc.* **1984**, *106*, 3492. (c) Kober, E. M.; Caspar, J. V.; Lumpkin, R. S.; Meyer, T. J. *J. Phys. Chem.* **1986**, *90*, 3722.

(7) (a) Sullivan, B. P.; Caspar, J. V.; Johnson, S. R.; Meyer, T. J. *Organometallics* **1984**, *3*, 1241. (b) Caspar, J. V.; Sullivan, B. P.; Meyer, T. J. *Organometallics* **1983**, *2*, 551. (c) Sullivan, B. P.; Smythe, R. S.; Kober, E. M.; Meyer, T. J. *J. Am. Chem. Soc.* **1982**, *104*, 4701.

(8) (a) Caspar, J. V. Ph.D. Dissertation, The University of North Carolina at Chapel Hill, 1982. (b) Kober, E. M.; Caspar, J. V.; Sullivan, B. P.; Meyer, T. J. *Inorg. Chem.* **1988**, *27*, 4587.

(9) Sullivan, B. P.; Salmon, D. J.; Meyer, T. J. *Inorg. Chem.* **1978**, *17*, 3334.

(10) Johnson, E. C.; Sullivan, B. P.; Salmon, D. J.; Adeyemi, S. A.; Meyer, T. J. *Inorg. Chem.* **1978**, *17*, 2211.

(11) Megehee, E. G. Ph.D. Dissertation, The University of North Carolina at Chapel Hill, 1986.

(12) Kelly, J. M.; Vos, J. G. *Angew. Chem., Int. Ed. Engl.* **1982**, *21*, 628.

(13) Parker, C. A.; Rees, W. T. *Analyst (London)* **1960**, *85*, 587.

(14) Caspar, J. V.; Meyer, T. J. *Inorg. Chem.* **1983**, *22*, 2444.

(15) Lumpkin, R. S.; Meyer, T. J. *J. Phys. Chem.* **1986**, *90*, 5307.

side of the spectral profile. The vibrational spacing $\hbar\omega_M$ was taken to be the energy difference between the resolved vibronic components, and S_M was estimated from the ratio of peak heights for the two highest energy vibronic components. Estimates of $\hbar\omega_L$ and S_L were not directly obtainable from the spectra. These three parameters were varied so as to obtain the best fits at low temperature, with $\hbar\omega_L = 350$ cm^{-1} and $S_L = 2.0$ being typical values chosen initially. These parameters are badly convoluted with $\Delta\bar{\nu}_{1/2}$. The low-temperature value for $\hbar\omega_L$ was held fixed throughout the temperature range so that any changes in the low-frequency mode with temperature are constrained to appear in S_L. A variety of combinations of $\hbar\omega_L$ (from 300 to 500 cm^{-1}) and S_L gave reasonable fits, although it was usually possible to obtain a best fit for a given value of S_L and $\hbar\omega_L$. When a best fit was determined at 80 K, $\hbar\omega_L$ was left fixed at that value in the temperature-dependent fits. This procedure constrains temperature-dependent contributions from the averaged low-frequency mode to appear in S_L.

Results

Photochemistry. Visible photolysis of the complexes $[(bpy)_2M(CO)X]^+$ (M = Os, Ru; X = H, D) in a variety of coordinating and noncoordinating solvents including acetonitrile (CH_3CN), dimethylformamide (DMF), acetone, propylene carbonate (PC), dimethyl sulfoxide (DMSO), ethanol (EtOH), and methanol (MeOH) showed the complexes to be photoinert even in the presence of the potential ligands PPh_3, Cl^-, or PhC≡CH. For *cis*-$[(bpy)_2Os(CO)X]^+$ (X = H, Cl), quantum yields for ligand loss in acetonitrile with Cl^- added as an entering group (2 mM $[N(n\text{-}C_4H_9)_4]Cl$) are immeasurable with $\phi_p < 2 \times 10^{-4}$. Under these conditions loss of bpy from $[Ru(bpy)_3]^{2+}$ occurs with $\phi_p = 0.029$.[16] The complex $[(bpy)_2Ru(CO)H]^+$ does undergo inefficient photochemical loss of CO with $\phi_p \leq 2 \times 10^{-3}$ under the same conditions. Our observations are consistent with those of Kelly and Vos for 365-nm photolysis of $[(bpy)_2Ru(CO)H]^+$ in CH_3CN.[17] One exception to the general absence of photochemistry in the presence of potential ligands was the relatively efficient conversion of $[(bpy)_2Os(CO)H]^+$ into $[(bpy)_2Os(CO)Cl]^+$ in CH_2Cl_2 in the presence of excess PPh_3. This reaction does not occur in the absence of PPh_3 and is probably induced by initial reductive quenching of the MLCT excited state by PPh_3.

Net photochemistry can also be induced by oxidative quenching. Photolyses in the presence of the oxidative quencher paraquat (PQ^{2+}) in CH_3CN rapidly resulted in an intense blue solution due to the appearance of the paraquat radical cation (PQ^+), as demonstrated by the appearance of a characteristic absorption feature near 600 nm. Aerial oxidation of PQ^+ to PQ^{2+} and spectroscopic

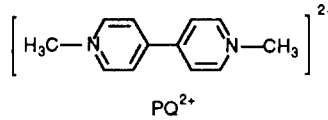

PQ^{2+}

analysis showed that the solvento complex *cis*-$[(bpy)_2Os(CO)(CH_3CN)]^{2+}$ was also a product of the photochemical reaction and that it was formed quantitatively. One-electron electrochemical oxidation of *cis*-$[(bpy)_2Os(CO)H]^+$ in acetonitrile also gives the solvento complex quantitatively, and H_2 appears as a coproduct, as shown by gas chromatography. The photochemistry in the presence of PQ^{2+}, no doubt, involves initial oxidative quenching of the Os–bpy MLCT excited state followed by redox decomposition of the Os^{III} hydrido complex (reaction 3).

$$[(bpy)_2Os^{II}(CO)H]^+ \xrightarrow{h\nu} [(bpy^{\bullet-})(bpy)Os^{III}(CO)H]^{+*} \quad (3a)$$

$$[(bpy^{\bullet-})(bpy)Os^{III}(CO)H]^{+*} + PQ^{2+} \rightarrow [(bpy)_2Os^{III}(CO)H]^{2+} + PQ^+ \quad (3b)$$

$$[(bpy)_2Os^{III}(CO)H]^{2+} + CH_3CN \rightarrow [(bpy)_2Os^{II}(CO)(CH_3CN)]^{2+} + \tfrac{1}{2}H_2 \quad (3c)$$

Table I. Excited-State Decay Parameters in 4:1 (v:v) Ethanol/Methanol at 25 °C

complex[a]	ϕ_{em}[b]	τ,[c] ns	k_r,[b] s^{-1}	k_{nr},[c] s^{-1}
$[Os(bpy)_3]^{2+}$[d]	0.0066	50	1.2×10^5	1.90×10^7
$[(bpy)_2Os(CO)H]^+$	0.0002	30	6.7×10^3[e]	3.33×10^7
$[(bpy)_2Os(CO)D]^+$	0.00042	55	7.6×10^3[e]	1.82×10^7
$[(bpy)_2Os(CO)Cl]^+$	0.0031	58	5.3×10^4	1.72×10^7
$[(bpy)_2Os(CO)py]^{2+}$[d]	0.11	1430	7.69×10^4	6.2×10^5

[a] As PF_6^- salts. [b] ±20%. [c] ±5%. [d] From ref 16. [e] This quantity is ηk_r, and η may not be unity. See the text and eq 5.

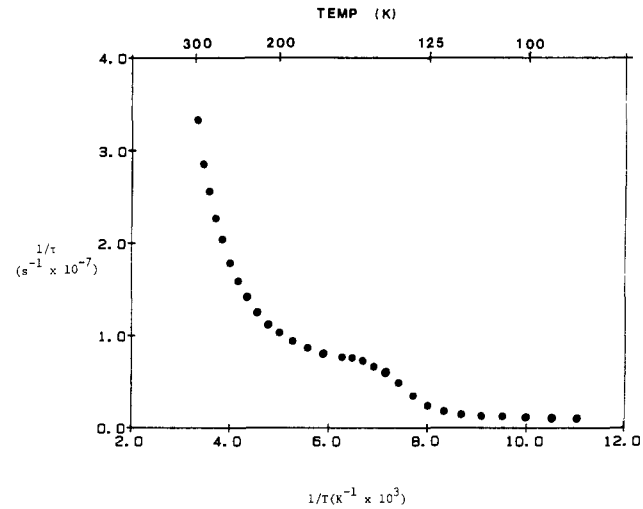

Figure 1. Temperature-dependent lifetime data for $[(bpy)_2Os(CO)H]PF_6$ (1.2×10^{-4} M) in 4:1 (v:v) ethanol/methanol from 90 to 298 K.

An inefficient M–H insertion photochemistry appears with added CS_2. Visible photolysis of $[(bpy)_2Os(CO)H]^+$ in 1:4 (v:v) CS_2/acetone for 2 days or of $[(bpy)_2Ru(CO)H]^+$ for 18 h gave the thioformyl CS_2 insertion products $[(bpy)_2(CO)MSC(=S)H]^+$.[11] This relatively inefficient photochemistry is in contrast to that of $[(bpy)Re(CO)_3H]$, where rapid insertion of CS_2 into the Re–H bond is known to occur at room temperature.[19]

Photophysical Properties. Emission quantum yields are listed in Table I. Radiative (k_r) and nonradiative (k_{nr}) decay rate constants were calculated from lifetimes (τ_0) and quantum yields (ϕ_{em}) by using eq 4 and 5. In eq 5, η is the efficiency with which

$$1/\tau_0 = k_r + k_{nr} \quad (4)$$

$$\phi_{em} = \eta k_r \tau_0 \approx k_r \tau_0 \quad (5)$$

the emitting excited state is reached. It is usually assumed to be unity for MLCT excited states.[20] For the hydrido complexes $[(bpy)_2Os(CO)X]^+$ (X = H, D), the calculated values for k_r are lower by a factor of ~10 than for the related complexes in Table I. One possible explanation for the decrease is that the k_r values themselves are normal, at ~10^5 s^{-1}, but that η is significantly less than 1.

Excited-state lifetimes were measured as a function of temperature by luminescence decay measurements following laser flash excitation into the lowest lying, intense MLCT transition for each complex. Temperature-dependent lifetime data were obtained in 4:1 (v:v) EtOH/MeOH from 90 K to room temperature for $[(bpy)_2Os(CO)X]^+$ (X = H, D, Cl) and from 90 to ~200 K for

(16) Allen, G. H.; White, R.; Rillema, D. P.; Meyer, T. J. *J. Am. Chem. Soc.* **1984**, *106*, 2613.
(17) Kelly, J. M.; O'Connell, C. M.; Vos, J. G. *J. Chem. Soc., Dalton Trans.* **1986**, 253.
(18) Danielson, E.; Lumpkin, R. S.; Meyer, T. J. *J. Phys. Chem.* **1987**, *91*, 1305.
(19) (a) Sullivan, B. P.; Meyer, T. J. *Organometallics* **1986**, *5*, 1500. (b) Sullivan, B. P.; Meyer, T. J. *J. Chem. Soc., Chem. Commun.* **1984**, 1244.
(20) Demas, J. N.; Taylor, D. G. *Inorg. Chem.* **1979**, *18*, 3177.
(21) (a) VanHouten, J.; Watts, R. J. *Inorg. Chem.* **1978**, *17*, 3381. (b) VanHouten, J.; Watts, R. J. *J. Am. Chem. Soc.* **1976**, *98*, 4853. (c) Durham, B.; Caspar, J. V.; Nagle, J. K.; Meyer, T. J. *J. Am. Chem. Soc.* **1982**, *104*, 4803. (d) Wacholtz, W. M.; Auerbach, R. S.; Schmehl, R. H.; Ollino, M.; Cherry, W. R. *Inorg. Chem.* **1985**, *24*, 1758. (e) Pinnick, D. V.; Durham, B. *Inorg. Chem.* **1984**, *23*, 3841.
(22) Lumpkin, R. S.; Kober, E. M.; Worl, L.; Murtaza, Z.; Meyer, T. J. *J. Phys. Chem.*, in press.

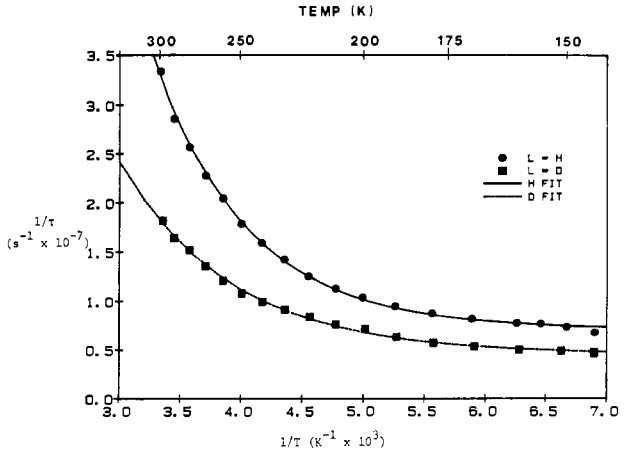

Figure 2. Plots of $1/\tau$ vs $1/T$ in fluid 4:1 (v:v) ethanol/methanol solution from 145 to 298 K for (●, —) $[(bpy)_2Os(CO)H]PF_6$ (1.2×10^{-4} M) and (■, ---) $[(bpy)_2Os(CO)D]PF_6$ (1.0×10^{-4} M). The symbols are the actual data points, and the lines are the nonlinear least-squares fits of the data to eq 6.

$[(bpy)_2Ru(CO)X]^+$ (X = H, D).

As shown by the data in Figure 1 for $[(bpy)_2Os(CO)H]^+$, there are three distinct regions of temperature-dependent behavior: (1) the low-temperature glass region (90–115 K), where the lifetime is nearly temperature independent; (2) the glass to fluid transition region (115–140 K), where the lifetime decreases rapidly with increasing temperature; (3) the fluid region (150–298 K), where $1/\tau$ decreases roughly exponentially as a function of $1/T$.

Previous temperature-dependent studies on tris(polypyridyl) complexes of Os(II) have shown that emission at 77 K is predominately from the third of three low-lying MLCT excited states with a small contribution (≤10%) from a second MLCT excited state.[4,23] The increase in lifetime as a function of temperature in the glass to fluid transition region is a result of the change in time scale for solvent dipole reorientations as the glass softens.[5d,18,24,25] The temperature dependence of τ for the complexes $[(bpy)_2Os(CO)X]^+$ (X = H, D, Cl) and $[(bpy)_2Ru(CO)X]^+$ (X = H, D) in the fluid region above 145 K can be successfully fit to eq 6.[31] Temperature-dependent behavior of this type is commonly observed for MLCT excited states of Ru(II) or Os(II).[3b,21,22]

$$1/\tau(T) = k + k' \exp(-\Delta E'/k_B T) \quad (6)$$

The appearance of the temperature-dependent term has been attributed to thermal population and decay from higher dd or MLCT excited states. In eq 6, k is the Boltzmann averaged sum of the radiative (k_r) and nonradiative (k_{nr}) rate constants (eq 7)

$$k = k_r + k_{nr} \quad (7)$$

for excited-state decay from the low-lying MLCT states. Since the complexes are weak emitters, $k_r \ll k_{nr}$ and $k \approx k_{nr}$.

When the temperature-dependent lifetime data are treated according to eq 6, any temperature dependence in k is forced into the exponential term. The relative independence of $1/\tau$ from T just past the glass to fluid transition region in Figure 1 suggests that k is, in fact, relatively independent of temperature.

Plots of $1/\tau$ vs $1/T$ in 4:1 (v:v) EtOH/MeOH for $[(bpy)_2Os(CO)H]^+$ and $[(bpy)_2Os(CO)D]^+$ are shown in Figure 2. In Table II, kinetic parameters obtained by fitting the temperature-dependent lifetime data to eq 6 are given for these complexes along with the 90 K lifetimes. Data for $[M(bpy)_3]^{2+}$ (M = Ru, Os) are included for comparison. The kinetic parameters were calculated by using an iterative nonlinear least-squares regression procedure.

Table II. Kinetic Parameters for Excited-State Decay in 4:1 (v:v) Ethanol/Methanol According to Eq 6

complex[a]	k,[b] s^{-1}	k',[c] s^{-1}	$\Delta E'$,[b] cm^{-1}	τ(90 K),[b] μs
$[(bpy)_2Os(CO)H]^+$	7.04×10^6	18.1×10^8	890	0.94
$[(bpy)_2Os(CO)D]^+$	4.49×10^6	5.08×10^8	750	1.32
$[(bpy)_2Os(CO)Cl]^+$	7.34×10^6	2.73×10^8	690	0.93
$[Os(bpy)_3]^{2+}$ [d]	3.70×10^6	0.76×10^8	330	0.77
$[(bpy)_2Ru(CO)H]^+$	6.78×10^5	1.05×10^{14}	1870	10
$[(bpy)_2Ru(CO)D]^+$	1.35×10^5	1.14×10^{13}	1665	18
$[Ru(bpy)_3]^{2+}$ [e]	4.1×10^5	4.5×10^{13}	3560	

[a] As PF_6^- salts. [b] ±5%. [c] ±10%. [d] Reference 26. [e] Reference 17.

Table III. Temperature Dependence of the Emission Spectra Fitting Parameters for $[(bpy)_2Os(CO)H]PF_6$ in 4:1 (v:v) Ethanol/Methanol[a,b]

T, K	E_{00}, cm^{-1}	S_M	S_L	$\Delta\bar{\nu}_{1/2}$, cm^{-1}	E_{em}, cm^{-1}	E_0, cm^{-1}
90	15800	1.05	2.10	600	15228	15265
95	15775	1.06	2.08	625	15195	
100	15735	1.05	2.05	650	15154	15191
105	15715	1.05	2.11	650	15117	15154
110	15675	1.04	2.12	675	15081	15117
115	15600	1.00	2.20	700	14933	15007
120	15475	0.92	2.50	750	14638	14785
125	15300	0.86	2.70	775	14342	14564
130	15150	0.80	2.95	775	14084	14342
135	15000	0.75	3.00	775	13936	14158
140	14875	0.76	2.85	800	13899	14084
150	14750	0.68	2.95	800	13752	13936
160	14675	0.71	2.75	825	13752	13899
170	14650	0.67	2.80	850	13678	13862
180	14625	0.65	2.75	875	13678	13862
200	14650	0.72	2.73	900	13678	
220	14650	0.72	2.75	950	13641	
240	14650	0.75	2.72	1000	13604	
260	14625	0.72	2.70	1050	13567	
280	14625	0.63	2.80	1100	13567	
300	14625	0.70	2.85	1200	13493	13826

[a] Calculated by using eq 1 with $\hbar\omega_M = 1250$ cm^{-1} and $\hbar\omega_L = 350$ cm^{-1}. [b] Error estimates: T, ±0.2 K; E_{00}, E_{em}, E_0, ±3%; $\hbar\omega_M$, S_M, ±5%; $\hbar\omega_L$, S_L, ±10%; $\Delta\bar{\nu}_{1/2}$, ±10%.

In Figure 3 are shown temperature-dependent emission spectra in 4:1 (v:v) EtOH/MeOH from 90 to 298 K for $[Os(bpy)_2(CO)H]PF_6$. The spectra have been normalized by arbitrarily setting the position of highest emission intensity to 1. These spectra illustrate the shift to lower energy that occurs through the glass to fluid transition from ~115 to 140 K and the nearly constant emission maxima above 170 K. The parameters derived from emission spectral fitting as a function of temperature are given in Table III for $[(bpy)_2Os(CO)H]^+$ and in Tables 1–3 in the supplementary material for $[(bpy)_2Os(CO)X]^+$ (X = D, Cl) and $[(bpy)_2Ru(CO)H]^+$. The results for all four complexes at 90 and 298 K are given in Table IV. Data are included in Table IV for $[Os(bpy)_3]^{2+}$ and $[(bpy)_2Os(CO)(py)]^{2+}$ [26] for comparison.

Discussion

It is evident from our photochemical studies that *cis*-$[(bpy)_2Os(CO)H]^+$ is essentially photochemically inert. The analogous Ru complex, $[(bpy)_2Ru(CO)H]^+$, does have a photochemistry, but it involves loss of CO and not the hydrido–Ru bond. Ligand-loss photochemistry is a common feature for polypyridyl complexes of Ru(II).[21] In many of the cases that have been studied in detail, the loss of a ligand occurs by initial MLCT excitation followed by thermal activation to a low-lying dd state. The loss

(23) (a) Lacky, D. E.; Pankuch, B. J.; Crosby, G. A. *J. Phys. Chem.* **1980**, *84*, 2068. (b) Allsopp, S. R.; Kemp, T. J.; Reed, W. J.; Carassiti, F.; Traverso, O. *J. Chem. Soc., Faraday Trans. 1* **1979**, *75*, 353. (c) Allsopp, S. R.; Kemp, T. J.; Reed, W. J. *J. Chem. Soc., Faraday Trans. 1* **1978**, *74*, 1275. (d) Hager, G. D.; Crosby, G. A. *J. Am. Chem. Soc.* **1975**, *97*, 7031. (e) Harrigan, R. W.; Hager, G. D.; Crosby, G. A. *Chem. Phys. Lett.* **1973**, *21*, 487. (f) Harrigan, R. W.; Crosby, G. A. *Chem. Phys.* **1973**, *59*, 3468.

(24) (a) Milder, S. J.; Gold, J. S.; Kliger, D. S. *J. Phys. Chem.* **1986**, *90*, 548. (b) Danielson, E.; Lumpkin, R. S.; Meyer, T. J. *J. Phys. Chem.* **1987**, *91*, 1305.

(25) Kein, H.-B.; Kitamura, N.; Tazuke, S. *Chem. Phys. Lett.* **1988**, *143*, 77.

(26) Lumpkin, R. S. Ph.D. Dissertation, The University of North Carolina at Chapel Hill, 1987.

Table IV. Emission Spectral Fitting Parameters at 90 and 298 K[a]

complex[b]	E_{00}, cm^{-1}	$\hbar\omega_M$, cm^{-1}	S_M	$\hbar\omega_L$, cm^{-1}	S_L	$\Delta\bar{\nu}_{1/2}$, cm^{-1}	E_0, cm^{-1}	$\Delta\bar{\nu}_{0,1/2}$, cm^{-1}
			90 K					
$[Os(bpy)_3]^{2+}$ [c]	14 300	1250	0.46	300	0.75	630	14 170	830
$[(bpy)_2Os(CO)H]^+$	15 800	1250	1.05	350	2.10	600	15 265	1260
$[(bpy)_2Os(CO)D]^+$	15 850	1250	1.02	350	2.17	600	15 300	1270
$[(bpy)_2Os(CO)Cl]^+$	17 175	1365	1.04	350	4.50	580	15 870	1730
$[(bpy)_2Os(CO)py]^{2+}$ [c]	19 280	1350	1.20	300	3.70	630	18 360	1400
$[(bpy)_2Ru(CO)H]^+$	17 750	1330	1.22	425	2.35	600	16 980	1560
			298 K					
$[Os(bpy)_3]^{2+}$ [c]	13 670	1250	0.60	300	0.75	1230	13 650	1480
$[(bpy)_2Os(CO)H]^+$	14 625	1250	0.70	350	2.85	1200	13 826	1940
$[(bpy)_2Os(CO)D]^+$	14 650	1250	0.65	350	2.78	1200	13 830	1960
$[(bpy)_2Os(CO)Cl]^+$	16 000	1365	0.53	350	5.65	1200	14 320	2510
$[(bpy)_2Os(CO)py]^{2+}$ [c]		1300	1.20				17 280	2070
$[(bpy)_2Ru(CO)H]^+$ [d]								

[a] In 4:1 (v:v) ethanol/methanol. [b] As PF_6^- salts. [c] Reference 26. [d] There is no emission from the complex at room temperature.

Table V. Excited-State Decay Parameters for $[(bpy)_2Os(CO)X]PF_6$ Complexes in 4:1 (v:v) Ethanol/Methanol at 25 °C

	298 K		90 K		298 K
complex	E_0, cm^{-1}	ln k_{nr}	E_0, cm^{-1}	ln k_{nr}(calc)	ln k_{nr}(calc)
$[Os(bpy)_3]^{2+}$ [b]	13 650	16.76	14 170	−26.48	−21.72
$[(bpy)_2Os(CO)H]^+$	13 826	17.32	15 270	−19.73	−19.94
$[(bpy)_2Os(CO)D]^+$	13 830	16.72	15 300	−20.10	−20.59
$[(bpy)_2Os(CO)Cl]^+$	14 320	16.67	15 870	−18.18	−20.13
$[(bpy)_2Os(CO)py]^{2+}$ [b]	17 280	13.34	18 330	−21.35	−20.11

[a] As PF_6^- salts. [b] Reference 18.

of the ligand occurs from the dd state.

Given their electronic structures, mechanisms appear to exist for these complexes that, in principle, could lead to photochemistry at the metal–hydrido bond. As shown by the quenching result in reaction 3, when oxidized to Os(III), $[(bpy)_2Os^{II}(CO)H]^+$ is unstable with regard to loss of the hydrido ligand as H_2. The change in electronic structure associated with the formation of the MLCT state involves a light-induced oxidation at the metal to give Ru^{III} or Os^{III} (eq 8). Since the excited states are stable,

$$[(bpy)_2M^{II}(CO)H]^+ \xrightarrow{h\nu} [(bpy)(bpy^{\bullet-})M^{III}(CO)H]^{+*} \quad (8)$$

the subsequent steps that lead to H_2 formation, as in reaction 3, must be too slow to compete with excited-state decay. Other possibilities for photodecomposition exist on the basis of initial MLCT excitation followed by intramolecular sensitization of excited states having different orbital origins. Those states include a hydrido → M(III) excited state, which could be reached by intramolecular electron transfer

$$[(bpy)(bpy^{\bullet-})(CO)M^{III}\text{–}H]^{+*} \rightarrow [(bpy)(bpy^{\bullet-})(CO)M^{II}\cdot H]^{+*}$$

or a σ–σ^*(M–H) excited state.

The speculation concerning mechanism is not inappropriate. It is known that in the related complexes of Re(I) $[(bpy)Re(CO)_3H]$[19] and $[(bpy)Re(CO)_3R]$[27] a relatively efficient Re–H or Re–R photochemistry does exist. The difference in behavior may lie, in part, in a difference in excited-state energetics. In electronically related complexes such as $[(bpy)_2Os(CO)Cl]^+$ and $[(bpy)Re(CO)_3Cl]$, the MLCT excited state based on Re^{II} is higher in energy by ~1000 cm^{-1} and more strongly oxidizing by 0.13 V. The increased oxidizing strength could lead to enhanced reactivity toward H_2 production via the MLCT state. The increase in the energy of the MLCT excited state could also lower the energy gap to σ–σ^*(M–H) or hydrido → M(III) excited states, making them more easily accessible by thermal activation following initial excitation at the MLCT chromophore.

Temperature-Dependent Lifetimes. Participation of Higher Energy States in Nonradiative Decay. At least three low-lying MLCT excited states are required to explain the temperature dependence of the emission intensity and lifetimes for polypyridyl complexes of Os(II) and Ru(II).[4,23,28] In the absence of a low-lying dd state or states, temperature-dependent studies have provided evidence for an additional MLCT state or states.[22,29] This state appears at higher energy and is shorter lived, apparently because of a higher degree of singlet character compared to the that in the lower MLCT states.[30]

The effective electronic symmetry at the metal in *cis*-$[(bpy)_2M(CO)H]^+$ (M = Ru, Os) is low, given the π-backbonding characteristics of the CO ligand and the σ-donor properties of the hydrido group:

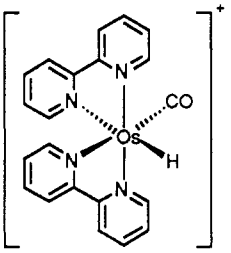

If electronic effects from the CO and H^- ligands are transmitted preferentially to the bpy ligands that lie mutually trans across the metal, a considerable splitting of the π^* levels could exist. The lowering of symmetry must create two parallel sets of MLCT states, each based on one of the two bpy ligands, which further complicates the MLCT excited-state structures of these complexes.

Although the electronic structures may be more complex, the temperature dependences of the lifetimes for the complexes $[(bpy)_2Os(CO)X]^+$ (X = H, D, Cl; Table II) can be interpreted, as in related complexes, as involving the population and decay

(27) Sullivan, B. P.; Thorpe, H. H.; Worl, L. Unpublished results.

(28) Hager, G. D.; Watts, R. J.; Crosby, G. A. *J. Am. Chem. Soc.* **1975**, *97*, 7037.

(29) Allen, G. H.; White, R. P.; Rillema, D. P.; Meyer, T. J. *J. Am. Chem. Soc.* **1984**, *106*, 2613.

(30) Kober, E. M.; Meyer, T. J. *Inorg. Chem.* **1984**, *23*, 3887.

(31) More generally, for two nondegenerate states for which there is an appreciable thermal population of the upper state, $1/\tau$ is given by the equation

$$1/\tau = \frac{k + k'\exp(-\Delta E'/k_BT)}{1 + \exp(-\Delta E'/k_BT)}$$

Azumi, T.; O'Donnell, C. M.; McGlynn, S. P. *J. Chem. Phys.* **1966**, *45*, 2735. Hager, G. D.; Crosby, G. A. *J. Am. Chem. Soc.* **1975**, *97*, 7031. Fits of the temperature-dependent lifetime data to this expression or to eq 6 gave equivalent results within experimental error.

(32) If zero-point energy and entropic differences are neglected, E_{00} is related to ΔE_{ES} by the equation[33]

$$\Delta E_{ES} = E_{00} + \chi_0$$

The quantity χ_0 is the solvent dipole reorganization energy for a transition between the states. It is related to the band width at half-maximum at room temperature by the expression

$$\Delta\bar{\nu}_{1/2}\ (\text{cm}^{-1}) = (2310\chi_0)^{1/2}$$

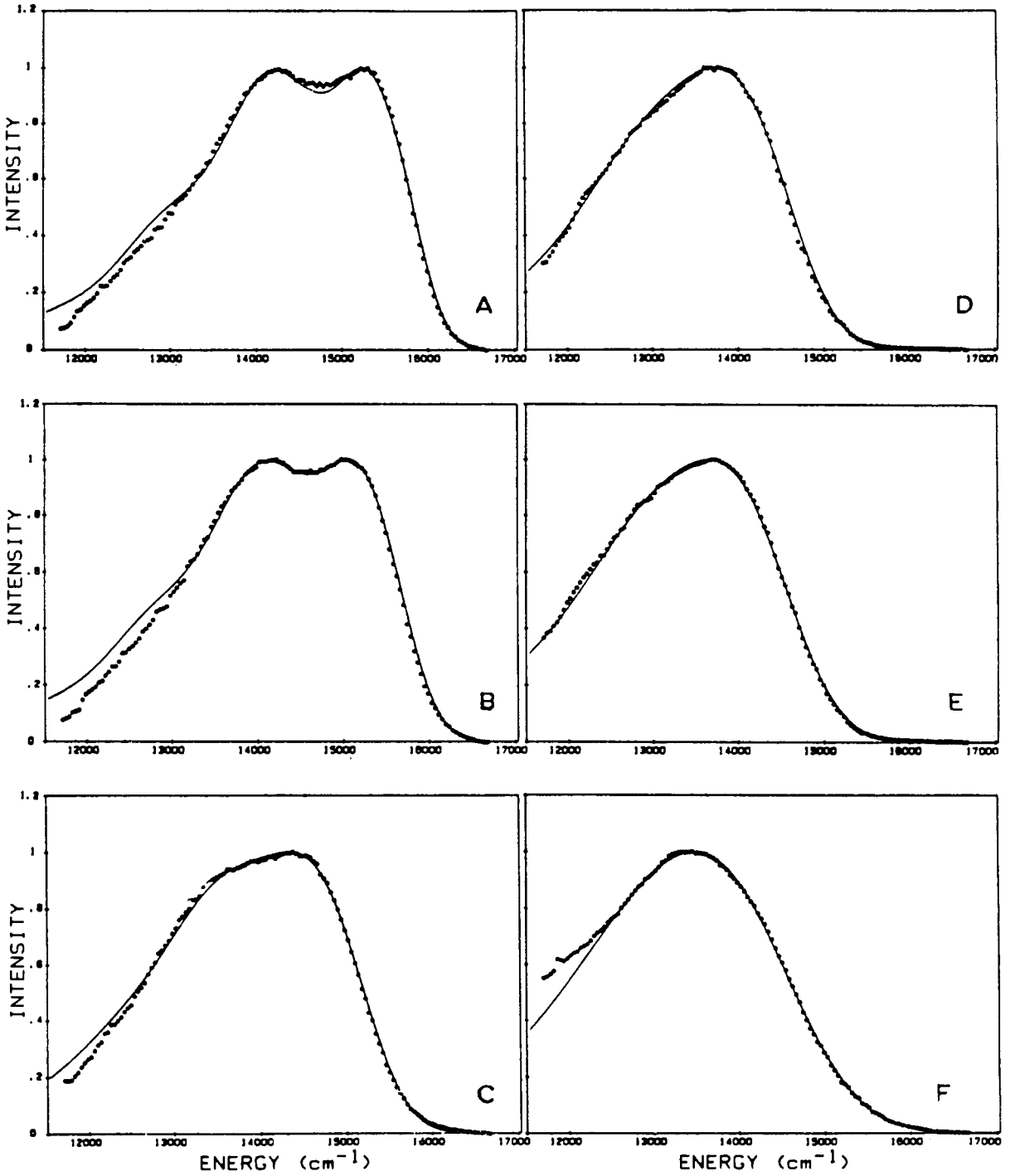

Figure 3. Emission spectra (✱) and spectral fits (—) for $[(bpy)_2Os(CO)H]PF_6$ in 4:1 (v:v) ethanol/methanol at (A) 90 K, (B) 110 K, (C) 125 K, (D) 150 K, (E) 200 K, and (F) 300 K.

of a higher MLCT state or states. With this interpretation, $k \approx k_{nr}$ in eq 6 includes the Boltzmann averaged contributions to nonradiative decay by the low-lying MLCT states. The parameter $\Delta E'$ ($\sim$800 cm^{-1}) is the energy gap to the higher lying MLCT state, and the preexponential term k' ($\sim 10^9$ s^{-1}) is the rate constant for decay from the higher MLCT state. Contributions to excited-state decay by the higher MLCT state or states are significant. They reach 50% of the total decay rate by room temperature for all of the cases studied here.

The temperature dependences of the lifetimes of the MLCT excited states of $[(bpy)_2Ru(CO)X]^+$ (X = H, D) are more profound. The magnitudes of the preexponential term ($k' = 10^{13}$–10^{14}) and the energy gap term ($\Delta E' \approx 1750 \pm 100$ cm^{-1}) are considerably greater than for Os. A contribution to the temperature dependence exists from thermal population and decay via a low-lying dd state or states. This is suggested by the appearance of the ligand-loss photochemistry. On the basis of a kinetic model for MLCT → dd decay that was developed for $[Ru(bpy)_3]^{2+}$,[3b,21] the magnitudes of k' and $\Delta E'$ suggest that they may be composite quantities in a kinetic sense. There may also be an additional contribution to these parameters from thermal population and decay via an additional MLCT state.

Emission Spectral Fitting Parameters. Excited-State Energetics and Structure. The parameters derived by emission spectral fitting—E_{00}, $\hbar\omega_M$, S_M, $\hbar\omega_L$, $\Delta\bar{\nu}_{1/2}$, E_0—give insight into the energetic and structural differences that exist between the excited and ground states. As noted in Results, S_M and $\hbar\omega_M$ are averaged quantities and include contributions from seven ν(bpy) modes. The quantities S_L and $\hbar\omega_L$ are averaged parameters for a series of low-frequency modes. The quantity $\Delta\bar{\nu}_{1/2}$ includes the contribution by the solvent.

For $[(bpy)_2Os(CO)X]^+$ (X = H, D), the emission spectral fitting parameters are comparable in magnitude to parameters found for related complexes.[6c,8a] Inspection of the data in Table

IV shows that there are no obvious consequences of the low electronic symmetry in $[(bpy)_2Os(CO)H]^+$ nor is there evidence of significant contributions to the emission spectral profile from the ν(Os—H) or ν(C≡O) modes. As suggested by the spectral fitting parameters for the hydrido and deuterio complexes, the emission spectra are independent of the replacement of H by D to within the error limits of the experiment.

There are some general trends that appear in the temperature-dependent data in Table III and in Tables 1–3 in the supplementary material. As the temperature is increased through the glass to fluid transition (~115–140 K), the energy gap between the ground and excited states (E_{00}) decreases as the glass softens and the average solvent dipole orientations around the excited state more closely approximate those of a fully fluid solution.[33] This is an expected result that has been observed previously for related complexes in the same medium.[18,26] Dynamic effects also exist.[5d,15,24,25] Above and below the glass to fluid transition, E_{00} is essentially temperature independent.

The electron-vibrational coupling constant S_M is proportional to the square of the difference in equilibrium displacement for the mode $\hbar\omega_M$ between the excited and ground states (eq 2). It decreases through the glass to fluid transition in parallel with E_{00}. Linear variations in S_M with energy gap have been observed when changes are made in the nonchromophoric ligands in the series $[(bpy)Os(L)_4]^{2+}$ and $[(phen)Os(L)_4]^{2+}$ (L = py, RCN, CO, PR_3, ...).[6c,8a,17] The observations of a decrease through the glass to fluid transition is important in showing that the fundamental basis for the change in the extent of distortion in the ν(bpy) modes is in the energy gap between the states and not in how the gap is varied. An increase in S_M with the energy gap is expected at least qualitatively.[6c,8a,17] As the energy gap is increased, the extent of ground-state–excited-state mixing is decreased and there is a greater degree of charge transfer in the excited state.

Additional Lifetime Effects. (1) Glass to Fluid Transition. Excited-state lifetimes for $[(bpy)_2Os(CO)X]^+$ (X = H, D, Cl) also decrease through the glass to fluid transition as the energy gap decreases (Figures 1 and 4). The variations are at least qualitatively consistent with a form of the energy gap law derived earlier for a related case.[15] For the limiting case where the acceptor role in nonradiative decay is played by a single, averaged, medium-frequency mode, an averaged low-frequency mode, and the solvent, the experimentally most useful form of the energy gap law is given in eq 9.[6c] In the derivation of eq 9 it was assumed

$$\ln k_{nr} = [\ln \beta - S_M + (\gamma + 1)^2(\Delta\bar{\nu}_{0,1/2}/\hbar\omega_M)^2/(16 \ln 2)] - \gamma E_0/\hbar\omega_M \quad (9)$$

$$\beta = (C_k^2\omega_k)(\pi/2\hbar\omega_M E_0)^{1/2} \qquad \gamma = \ln (E_0/S_M\hbar\omega_M)^{-1} \quad (10)$$

that $E_0 \gg \hbar\omega_M$ and that $S_M\hbar\omega_M \gg k_BT$. The averaged low-frequency mode is treated semiclassically, and the solvent is included through $\Delta\bar{\nu}_{0,1/2}$. The variables in eq 9 have the same meaning as defined previously. The term ω_k is the angular frequency or averaged frequency for the promoting mode or modes. If we assume that variations in β, S_M, and $(\gamma + 1)^2$ with E_0 are small, eq 9 simplifies to give eq 11. The quantity A in eq 11 is defined in eq 12.

$$\ln (1/\tau) \approx k_{nr} = A - \gamma E_0/\hbar\omega_M \quad (11)$$

$$A = \ln \beta - S_M + (\gamma + 1)^2(\Delta\bar{\nu}_{0,1/2}/\hbar\omega_M)^2/(16 \ln 2) \quad (12)$$

As shown in Figure 4, there is at least a qualitative linear variation of $\ln (1/\tau)$ with E_0 through the glass to fluid transition for the salts $[(bpy)_2Os(CO)X]PF_6$ (X = H, D, Cl). Because the spectra in this region include dynamical effects arising from solvent dipole reorientations,[5d,15,24,25] and the expected $T^{1/2}$ dependence of $\Delta\bar{\nu}_{0,1/2}$ is neglected, it is difficult to ascribe quantitative significance to the correlations. The slopes and intercepts of the lines are in reasonable agreement with values obtained earlier for related chromophores where the variation in E_0 (or E_{em}) was induced by changes in ligands,[6c,34] counterions,[35] solvent,[36] or the glass to fluid transition.[15]

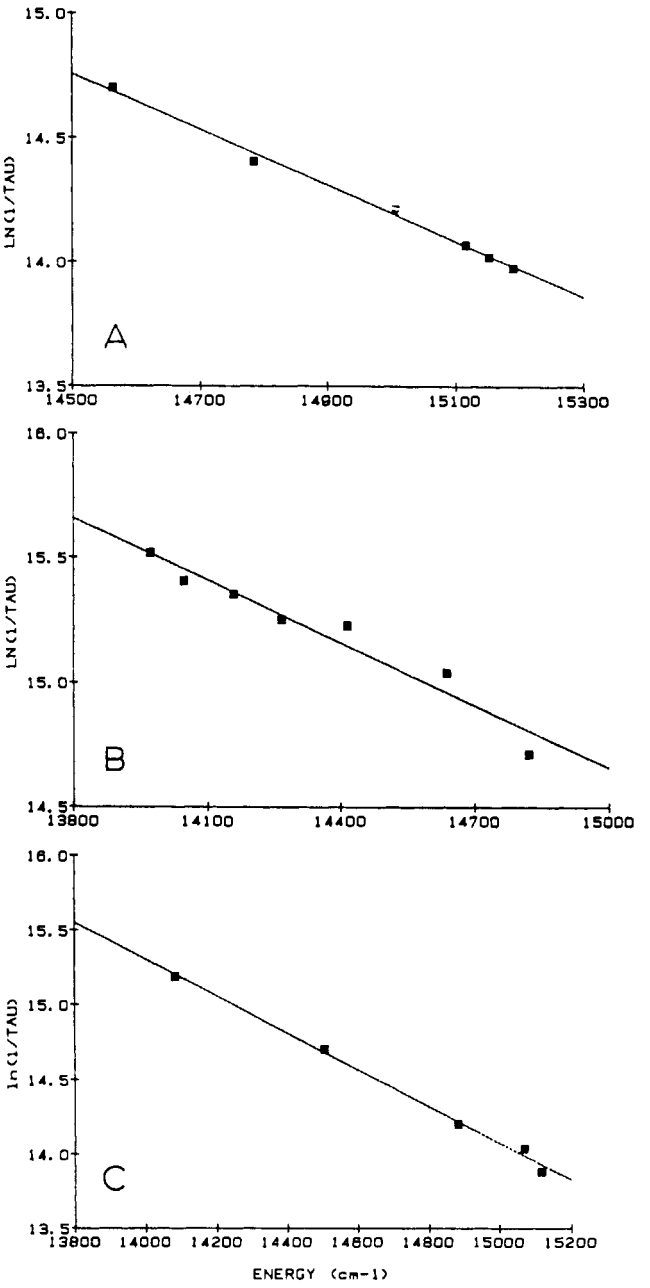

Figure 4. Plots of $\ln (1/\tau)$ vs E_0 for (A) $[(bpy)_2Os(CO)H]PF_6$, (B) $[(bpy)_2Os(CO)D]PF_6$, and (C) $[(bpy)_2Os(CO)Cl]PF_6$ through the glass to fluid transition region in 4:1 (v:v) ethanol/methanol. Squares are the actual data points, and the lines are the linear least-squares fits of the data to the energy gap law in eq 17. The respective slopes and intercepts of the lines drawn in the figure are as follows: (A) $(-1.23 \pm 0.05) \times 10^3$ cm^{-1}, 32.5 ± 0.7; (B) $(-0.84 \pm 0.09) \times 10^3$ cm^{-1}, 27.2 ± 1.3; (C) $(-1.12 \pm 0.04) \times 10^3$ cm^{-1}, 31.1 ± 0.6.

(2) Kinetic Isotope Effects. Role of the ν(M—H) Mode. In the limit of applicability of the energy gap law, the relative contributions of the various normal modes as energy acceptors depend upon both the change in equilibrium displacement through S and the quantum spacing, $h\nu = \hbar\omega$. They are the key parameters that dictate the relative magnitudes of the vibrational overlap integrals.

(33) Lumpkin, R. S.; Worl, L.; Kober, E. M.; Murtaza, Z.; Meyer, T. J. *J. Phys. Chem.*, in press.

(34) (a) Caspar, J. V.; Kober, E. M.; Sullivan, B. P.; Meyer, T. J. *J. Am. Chem. Soc.* **1982**, *104*, 630. (b) Barqawi, K.; Llobet, A.; Meyer, T. J. *J. Am. Chem. Soc.* **1988**, *110*, 7751.

(35) Vining, W. J.; Caspar, J. V.; Meyer, T. J. *J. Phys. Chem.* **1985**, *89*, 1095.

(36) Caspar, J. V.; Sullivan, B. P.; Kober, E. M.; Meyer, T. J. *Chem. Phys. Lett.* **1982**, *91*, 91.

The ν(Os—H) modes is of relatively high energy (ν(Os—H) = 2015 cm^{-1}; ν(Os—D) = 1425 cm^{-1}). Given the change in oxidation state at the metal in the excited state (eq 8), it seemed reasonable to expect that a significant role in nonradiative decay would be played by this mode. However, the low-temperature emission spectra of $[(bpy)_2Os(CO)H]PF_6$ and $[(bpy)_2Os(CO)D]PF_6$ are essentially superimposable and the k_H/k_D kinetic isotope for nonradiative decay is small (Table II).

It is possible to derive a modified form of the energy gap law equation that includes a contribution from ν(M—H). In the limit that such a contribution does exist but that the energy-accepting role continues to be dominated by the averaged, medium-frequency ν(bpy) mode, $S_H\hbar\omega_H \ll S_M\hbar\omega_M$, the expression for ln k_{nr} is given in eq 13.[11,37] In eq 13, $\chi_M = S_M\hbar\omega_M$, A was defined in eq 12,

$$\ln k_{nr} \approx A - \gamma E_0/\hbar\omega_M + S_H(E_0/\chi_M)^{\omega_H/\omega_M} \quad (13)$$

and S_H and $\hbar\omega_H$ are the electron-vibrational coupling constant and quantum spacing for the M—H mode. The ratio of the nonradiative decay rate constants for the protio and deuterio complexes, ln (k^H_{nr}/k^D_{nr}), is given by eq 14. In this derivation,

$$\ln (k^H_{nr}/k^D_{nr}) \approx S_H(E_0/\chi_M)^{\omega_H/\omega_M} - S_D(E_0/\chi_M)^{\omega_D/\omega_M} \quad (14)$$

$S_H = S_D$ since S is a measure of the potential curve for the oscillator. With this result it is possible to derive an expression relating S_H to the experimentally observed kinetic isotope effect, eq 15. By use of the appropriate values for k_{nr}, ω_D or ω_H, E_0,

$$S_H = \frac{\ln (k^H_{nr}/k^D_{nr})}{(E_0/\chi_M)^{\omega_H/\omega_M} - (\omega_H/\omega_D)(E_0/\chi_M)^{\omega_D/\omega_M}} \quad (15)$$

and χ_M, $S_H = 0.011$ for $[(bpy)_2Os(CO)H]^+$. The change in equilibrium displacement, ΔQ_e, can be calculated from S_H, ω_H, and the reduced mass, M_H, by eq 16. This calculation gives ΔQ_e

$$S_H = (M_H\omega_H/2\hbar)(\Delta Q_e)^2 \quad (16)$$

= 0.019 Å. The small change in equilibrium displacement for the ν(Os—H) mode between the MLCT excited state and the ground state is consistent with the absence of significant contributions from ν(Os—H) to the emission spectrum or energy gap correlations.

On the other hand, from the data in Table II, k^H_{nr}/k^D_{nr} (=5.02) is significant for $[(bpy)_2Ru(CO)X]^+$ (X = H, D). Because these complexes are such weak emitters, the emission spectral fitting procedure could only be extended to 170 K for $[(bpy)_2Ru(CO)H]^+$ and lifetime data are available only to 185 K. Past the glass to fluid transition these parameters typically remain relatively constant (Table 3 in the supplementary material), except for the bandwidth, which increases with $T^{1/2}$ as expected. By use of parameters obtained above the glass to fluid transition—E_0 = 15 400 cm^{-1}, S_M = 1.12, $\hbar\omega_M$ = 1350 cm^{-1}, $\hbar\omega$(Ru—H) = 2015 ± 50 cm^{-1}—eq 15 gives S_H(Ru—H) = 0.037 ± 0.004. This value for S_H leads to a change in equilibrium displacement of ΔQ_e(Ru—H) = 0.035 ± 0.002 Å and a respectable contribution of ν(Ru—H) to nonradiative decay.

The appearance of a greater distortion for the M—H bond in the excited state of the Ru complex may be an important observation. The estimated bond length change is apparently not sufficient to affect the chemical reactivity of the M—H bond in the excited state, but it could represent a trend that leads to reactivity. The increase is presumably a consequence of the greater oxidizing strength of the Ru^{III} center in the $(bpy^{\bullet-})Ru^{III}$ MLCT excited state compared to that of Os^{III} in $(bpy^{\bullet-})Os^{III}$. The redox potential of the M(III) site in the excited state is related to the ground-state, ligand-based reduction potential, $E°'(M^{II}(bpy)/M^{II}(bpy^{\bullet-}))$, and the internal energy difference between the ground and excited states, ΔE_{ES}, by eq 17.[32] By use of eq 17, the

$$E°'(M^{III}(bpy^{\bullet-})/M^{II}(bpy^{\bullet-})) \approx \Delta E_{ES} + E°'(M^{II}(bpy)/M^{II}(bpy^{\bullet-})) \quad (17)$$

Ru-based excited state is a stronger oxidant by ~0.3 V than is the Os-based excited state. The greater oxidizing strength comes primarily from the ~2000 cm^{-1} higher energy of the Ru-based excited state (Table IV). The increased energy gap leads to a decreased mixing of the excited and ground states and greater charge-transfer character in the excited state. Since the Ru(III) site is more electron deficient, there is a greater polarization of the M—H bond toward Ru(III) and a shorter Ru—H bond length in the MLCT excited state.

From the temperature-dependent lifetime data, the exchange of D for H in the hydrido complexes has an effect on $\Delta E'$, but the difference is within the experimental uncertainty in $\Delta E'$ in both cases. The isotope effect appears mainly in the preexponential term, k', with $k_H'/k_D' = 3.6$ for Os and $k_H'/k_D' = 9.2$ for Ru. If the term $k'\exp[-(\Delta E'/RT)]$ arises from nonradiative decay from a higher MLCT state for $[(bpy)_2Os(CO)H]^+$, the H/D kinetic isotope effect may signal a change in dπ orbital composition for this state. The isotope effect on k' for the Ru case must reflect, at least in part, the dynamics of a MLCT → dd surface crossing. The appearance of such a large, temperature-independent effect is consistent with a significant change in equilibrium displacement in ν(Ru—H) between the MLCT and dd states with a significant contribution to the transition between states arising from nuclear tunneling.

Acknowledgments are made to the U.S. Department of Energy under Grant No. DE-AS05-78ER06034 for support of this work and to Dr. E. M. Kober for invaluable assistance with the spectral fitting program and with the modification to the energy gap law to include an additional high-frequency mode.

Registry No. $[(bpy)_2Os(CO)H]^+$, 84117-35-1; $[(bpy)_2Os(CO)D]^+$, 122520-48-3; $[(bpy)_2Os(CO)Cl]^+$, 80502-54-1; $[(bpy)_2Ru(CO)H]^+$, 82414-89-9; $[(bpy)_2Ru(CO)D]^+$, 122520-50-7.

Supplementary Material Available: Listings of the temperature dependence of emission spectral fitting parameters for $[(bpy)_2Os(CO)D]PF_6$, $[(bpy)_2Os(CO)Cl]PF_6$, and $[(bpy)_2Ru(CO)H]PF_6$ (3 pages). Ordering information is given on any current masthead page.

(37) Kober, E. M. Manuscript in preparation.